ORIGINAL PAPER

THE EFFECT OF ELECTROLYTE COMPOSITIONS ON THE STRUCTURE AND PROPERTIES OF PEO COATINGS ON PURE Ti SUBSTRATE

ELISABETA COACA[1], VICTOR AUREL ANDREI[2,3], IOANA DANIELA DULAMA[3], ANDREEA LAURA BANICA[3,4], CRISTIANA RADULESCU[3,4,5,*], CRISTIAN MIHAILESCU[6]

Manuscript received: 07.11.2022; Accepted paper: 14.01.2023; Published online: 30.03.2023.

Abstract. *Plasma electrolytic oxidation method was used to form ceramic coatings on pure Ti substrates, using various aqueous solutions of sodium aluminate (15 g/L and 20 g/L, with or without the addition of NaOH, 2 g/L). The PEO process was carried out at constant time and voltage (300 seconds, 200 V). The ceramic coatings obtained by PEO were investigated by SEM, EDS, XRD, and XPS. Their corrosion behavior has been evaluated as well. The study aimed to understand the role of NaOH in the development of the PEO process and to evaluate the results obtained by short treatments in potentiostatic regime.*

Keywords: *CP-Ti corrosion resistance; plasma electrolysis oxidation; X-ray photoelectron spectroscopy; scanning electron microscopy; X-ray diffraction; energy dispersive X-ray spectrometry*

1. INTRODUCTION

Titanium (Ti) and its alloys have remarkable properties including high corrosion resistance, good mechanical behavior, good fatigue strength and toughness, low elastic modulus, high strength-to-weight ratio, relatively low density, high melting point, good biocompatibility. These properties have led to the development of a wide range of industrial applications in various fields as nuclear, aerospace, chemical, biomedical, automotive, energy, military, and marine. In addition, titanium and its alloys are extensively used in the nuclear industry from condensers in power plants to electrolytic dissolvers in reprocessing plants [1, 2]. Although titanium offers excellent corrosion resistance, it suffers from biofouling characteristics in seawater environments. Some drawbacks related to low wear resistance, low hardness, high coefficient of friction and poor corrosion resistance in aggressive environments such as sulfuric acid, hydrochloric acid and phosphoric acid are among the factors that can limit the applications of these alloys. Different methods such as electrodeposition, laser cladding, thermal spray, plasma spray, plasma immersion implantation, physical and chemical

[1] Institute for Nuclear Research Pitesti, 115400 Mioveni, Romania. E-mail: elisabetaandrei@yahoo.com.
[2] Elssa Laboratory SRL, 110109 Pitesti, Romania. E-mail: andvic12@yahoo.com.
[3] Valahia University of Targoviste, Institute of Multidisciplinary Research for Science and Technology, 130004 Targoviste, Romania. E-mail: dulama_id@yahoo.com.
[4] Politehnica University of Bucharest, Doctoral School of Chemical Engineering and Biotechnology, Bucharest, Romania. E-mail: banica_andreeal@yahoo.com.
[5] Valahia University of Targoviste, Faculty of Science and Arts, 130004 Targoviste, Romania.
E-mail: cristiana.radulescu@valahia.ro.
National Institute for Lasers, Plasma and Radiation Physics, 077125 Magurele, Romania.
E-mail: cristi.mihailescu@inflpr.ro.

vapor deposition (PVD and CVD), and conversion coatings can be used for improving the materials properties and composition, and thus form wear- and corrosion-resistant coatings. Titanium anodizing produces TiO_2 anatase films, which significantly reduce bacterial adhesion to near ultraviolet light. In high oxidation nitric acid environments, titanium suffers from excessive corrosion due to the condensation attack that generates a layer of white, weak and non-stick TiO_2. A double oxide coating for reconditioning of Ti formed through electrolytic anodic oxidation provides a corrosion resistant surface with minimum degradation [2]. Surface science and surface engineering are active areas of research in the development of materials with special properties for advanced technologies.

Plasma electrolytic oxidation (PEO) technique derived from traditional anodic oxidation has attracted recently considerable interest [3]; the PEO process is performed at higher voltages than the dielectric breakdown happens, at the same time as that taken for reaching the breakdown voltage. Consequently, plasma discharge channels, with local temperature range of 2000-10000 K, are formed; then, short-lived micro-discharges with incidence of light and gas emission are produced steadily across the coating surface during the coating growth. These events allow the oxide coating to be growth [3,4]

Composites of alumina (Al_2O_3) and titania (TiO_2) are known for their high toughness, low thermal expansion, and low thermal conductivity. Alumina-Titania coatings are excellent candidates for providing protection against abrasive wear, resistant to high temperature erosion with cryogenic compatibility, high adhesion strength, and are resistant to high thermal shock; high temperature formation of Al_2TiO_5 (AT) is reason for the excellent property [5].

Recently, the obtaining of advanced ceramic coatings by PEO on pure Ti substrate using aluminate-based electrolytes was investigated [3, 6-9]. The properties and structures of the coatings formed are determined by the PEO process parameters. In [7], the PEO process was carried out in 10 g/L and 5 g/L aqueous solutions of $NaAlO_2$ at constant time and voltage (180 seconds and 420 V) and all the coatings formed consisted in rutile, anatase and a small number of $TiAlO_5$ phases. Some studies [8, 9], described the oxidation process of Cp–Ti grade 2 substrates in galvanostatic regime, at constant current density j=0.36 A/cm^2, employing a unipolar, pulsed, direct-current power source at a frequency of 150 Hz, in electrolytic bath containing $NaAlO_2$ with different concentrations (10 g/L, 15 g/L and 20 g/L), with or without the addition of NaOH 2 g/L; in addition, the period of the applied PEO treatments were 10, 20 and 30 min. In the case of the addition of NaOH in the electrolysis bath, the coatings are polycrystalline showing titanium-aluminum oxides, in the form of $TiAl_2O_5$ and/or $Ti_2Al_6O_{13}$ as dominant phases, combined with γ–Al_2O_3 and α–Al_2O_3 forms and a small amount of $NaAl_6O_{9.5}$ crystal structure [8].

In the case of coatings prepared in electrolytic bath containing only $NaAlO_2$ is highlighted the presence in the coatings of aluminum oxide as a major component, the explanation being related to the lower electrical conductivity in the absence of added NaOH. This is why for an identical current density established in the galvanostatic regime, the actual values of the working voltages applied on the samples during the process were considerably higher than in the case of electrolytes with added NaOH. Because of this, in the outer layer, the higher working voltages reached during the PEO experiment produced a considerable temperature increase in the microarc electric discharge region, favoring the partial decomposition of $TiAl_2O_5$ (which is metastable) to TiO_2 and Al_2O_3. At the same time, aluminum oxide was subjected to phase transformation, leading to the formation of α- and γ-Al_2O_3 phases, while TiO_2 combined with Na_2O to form $Na_2Ti_4O_9$ ($Na_2O \cdot 4TiO_2$) [9].

The aim of this study was to assess the results obtained by short treatments in potentiostatic regime, and to understand the role of NaOH in the development of the PEO process.

2. MATERIALS AND METHODS

2.1. PREPARATION OF PEO COATINGS

CP-Ti grade 2 samples (11x25x3) mm^3, were manually grounded up to 1200 mesh SiC paper to achieve a fine finish with an average surface roughness of 0.35 mm, which minimizes the mechanical surface damage and allows a good adherence of coated layer [10]. Plasma electrolytic oxidation of CP-Ti grade 2 samples was performed using a unipolar pulsed DC power source with 150 Hz frequency [11]. Before carrying out PEO experiments the samples were cleaned by ultrasound treatment in ethanol and acetone for 20 min. Four aqueous sodium aluminate solutions were prepared using pure reagents and distilled water: E1 containing $NaAlO_2$ – 15 g/L (pH=12.8; k=18.0 mS/cm); E2 containing $NaAlO_2$ –15g/L and NaOH – 2 g/L (pH=13.1; k=26.0 mS/cm); E3 containing $NaAlO_2$ – 20 g/L (pH=13.0; k=22.5 mS/cm); E4 containing $NaAlO_2$ – 20 g/L and NaOH – 2 g/L (pH=13.1; k=29.8 mS/cm).

In the anodic oxidation process, the voltage was increased so that the intensity of the electric current through the electrolysis bath did not exceed 5 A, until the appearance of the electric discharge in the spark (Usd = 160V–180 V). From this moment the voltage was increased rapidly until reaching the value 200 V, at which the electric discharge was performed in the microarc. The duty cycle was fixed at 34%. Samples called S1, S2, S3, S4, were subjected for 5 minutes to PEO treatment, respectively in electrolytes E1, E2, E3, E4. During the process, current density decreasing due to film growth, varied in the range of 0.36-0.35 A/cm^2 for S1, 0.54-0.27 A/cm^2 for S2, 0.36-0.32 A/cm^2 for S3 and 0.63-0,27 A/cm^2 for S4. The electrolyte temperature was kept at values less than 15°C.

An advantage of the PEO technique is that it allows the treatment of samples with different shapes and sizes; the important parameter is the current density, the treatment of large samples requiring the use of high electric currents. The dimensions of the samples used in this study are suitable for the development of the treatment method, and for performing different analyzes to characterize the coatings made.

2.2. CHARACTERIZATION OF PEO COATINGS

The thicknesses of the oxide layers formed were determined by metallography. In this respect, the samples were cut into section with the Buehler Isomet 4000 device (Spectrographic Ltd., Leeds, UK), and then packed into a copper foil and mounted in a thermoplastic raisin with the Metapress-A covering press (Mark V Laboratory, Hartford, Connecticut, USA). After mounting, the sample was grinded and polished (120–2400 grained abrasive paper) with a Beta Grinder-Polisher (Buehler, Lake Bluff, Illinois, USA).

Scanning Electron Microscopy (SEM) and elements microanalysis analysis of surface morphology of PEO coatings and elemental analysis was performed using Scanning Electronic Microscope (SU-70, Hitachi, Tokyo, Japan) coupled with Energy Dispersive X-ray spectrometer (UltraDry, Thermo Fisher Scientific GmbH, Dreieich, Germany). The Thermo Scientific™ Pathfinder™ X-ray Microanalysis Software allows achieving the element distribution maps.

X–Ray Diffraction (XRD) analysis was used to examine the crystal composition of the oxide layers employing a Rigaku Ultima IV diffractometer (Rigaku, Tokyo, Japan), with Cu K_α radiation (40 KV, 30 mA). For the qualitative phase analysis, the X-ray diffractograms were obtained by scanning the (2θ) = 15–80° range with 0.05° step and 5 s step-time using Bragg-Brentano $(\theta - \theta)$ focusing scheme and graphite monochromator in diffracted beam.

X–ray Photoelectron Spectroscopy (XPS) analysis has been carried out to study the bonding state of atoms at the surface and to determine the surface composition. It has been used the Electron Spectrometer (ESCALAB 250, Thermo Fisher Scientific, Waltham, MA, USA) which ensures an energetic resolution smaller the 0.45 eV for XPS technique and facilitates localized spectroscopy (spot less than 120 µm). XPS spectra were recorded using Al Kα monochromatized source (hν=1486.6 eV) in a vacuum of 10^{-8} Pa. The acquired spectra were calibrated with respect of the C1s line of surface adventitious carbon at EB=284.8 eV (where EB represents the binding energy of the electron with respect to the vacuum level). An electron flood gun has been used to compensate the charging effect in insulating samples. The analyzed areas were cleaned by Ar ion beam etching. A delocalized Ar^+ ion beam accelerated under 2 keV was used to remove absorbed contaminants on the surfaces. Survey spectra were acquired in the following conditions: X-ray spot size=500 µm, number of scans=1, pass energy=100 eV, energy step size=1 eV. High resolution spectra were acquired on energy regions for Al 2p, O 1s, Ti 2p, Cr 2p, Na 1s peaks under the following conditions: X-ray spot size=500 µm, number of scans=50, pass energy=5 eV, energy step size=0.1 eV.

Potentiodynamic polarization measurements were performed on a potentiostat /galvanostat (ParStat-2273, Princeton Applied Research, Oak Ridge, Tennessee, USA) in a three-electrode set, including the working electrode (test sample), a graphite electrode and a saturated calomel Hg_2Cl_2 (0.244 V *vs*. SHE at 25°C). Polarization curves were obtained in 0.5 M NaCl aqueous electrolyte, at scan rate of 0.5 mV/s and in the range of -0.3 V – +1.0 V versus open circuit potential, step height 1 mV. The corrosion behavior was investigated using Tafel slope method.

3. RESULTS AND DISCUSSION

3.1 SURFACE MORPHOLOGY OF THE PEO COATINGS

Fig. 1 shows the thicknesses of the oxide layers determined by metallography; it is observed that by increasing the concentrations of $NaAlO_2$ and by adding NaOH, coatings with higher and more uniform thickness are obtained.

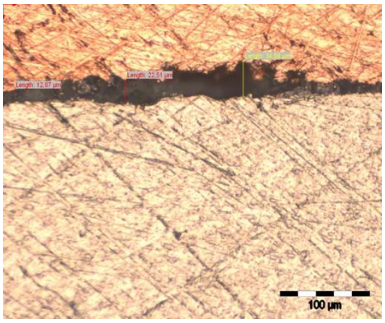

a) Sample S1; d= 12÷34 µm

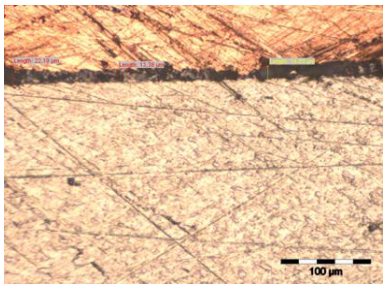

b) Sample S2; d= 14÷22 µm

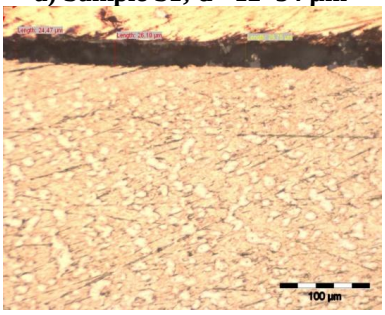

c) Sample S3; d= 24÷27 µm

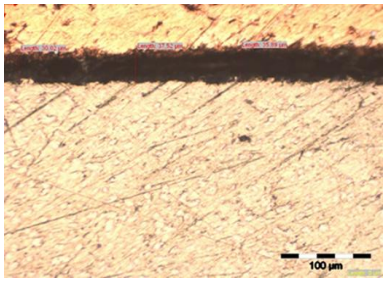

d) Sample S4; d= 30÷36 µm

Figure 1. The thicknesses of the oxide layers

The results obtained by SEM/EDS analysis are shown in Figs. 2-3 and Table 1 for sample S1, Figs. 4-5 and Table 2 for sample S2, Figs. 6-7 and Table 3 for sample S3 and Figs. 8-9 and Table 4 relating to sample S4.

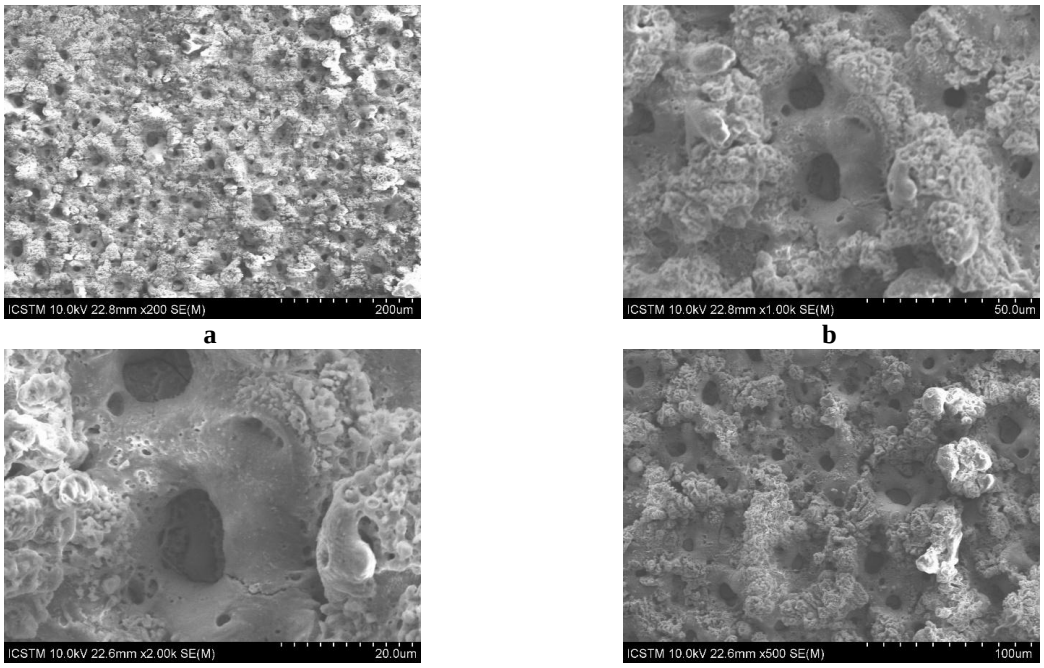

a **b**

c **d**

Figure 2. SEM photomicrographs of S1 sample: a) x200; b) x1000; c) x2000; d) impurities x500.

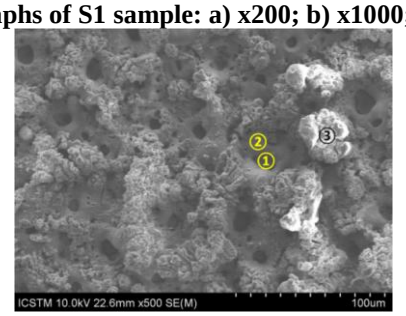

Figure 3. Points of S1 sample analyzed by EDS.

Table 1. The elemental composition determined by FE-SEM-EDS in the studied points of S1 sample, expressed in wt.% ± S.D.%, normalized to 100 wt.%.

Element [wt.%±S.D.%]	P1	P2	P3
Ti	89.16±1.38	14.17±0.17	6.59±0.15
Al	3.91±0.08	32.99±0.13	41.13±0.16
O	6.88±0.27	52.22±0.26	47.02±0.24
Na	0.06±0.02	0.61±0.02	5.26±0.04

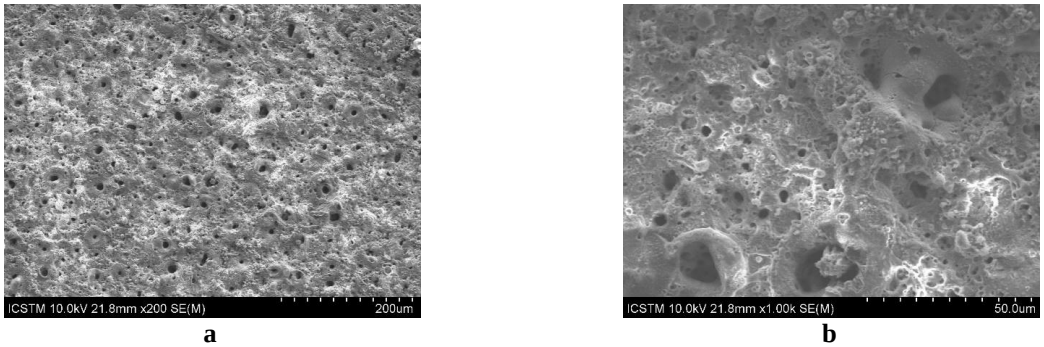

a **b**

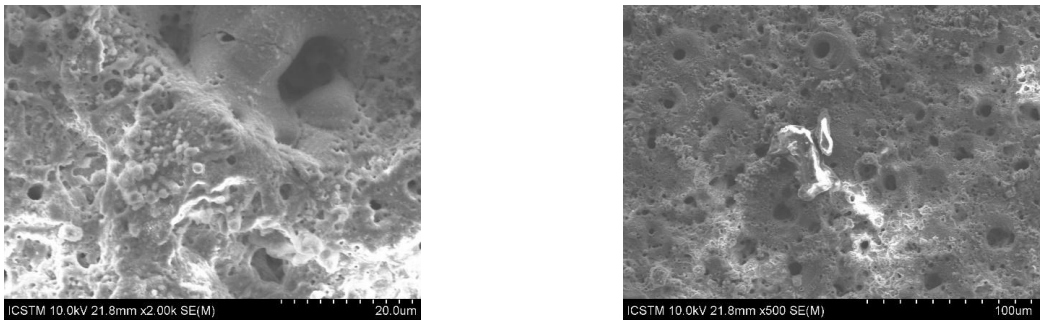

c **d**

Figure 4. SEM photomicrographs of S2 sample: a) x200; b) x1000; c) x2000; d) area with crystalline grains x500.

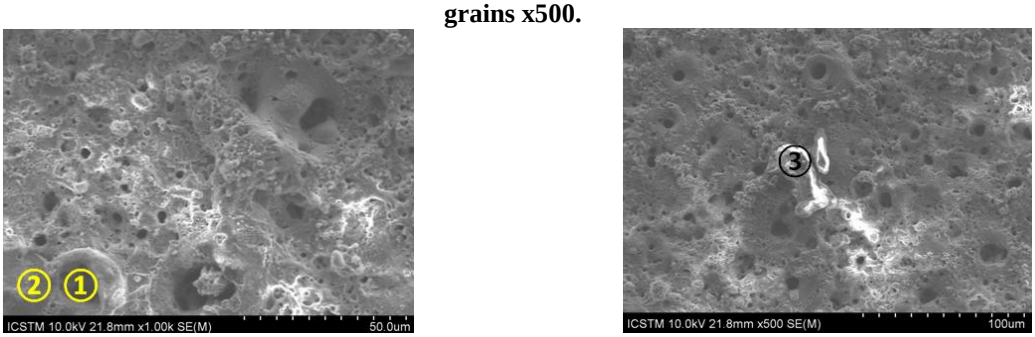

Figure 5. Points of S2 sample analyzed by EDS.

Table 2. The elemental composition determined by FE-SEM-EDS in the studied points of S2 sample, expressed in wt.% ± S.D.%, normalized to 100 wt.%.

Element [wt.%±S.D.%]	P1	P2	P3
Ti	83.75±1.10	31.23±0.65	1.59±0.69
Al	11.26±0.11	52.57±0.25	11.56±0.50
O	4.89±0.16	15.60±0.19	81.89±0.71
Na	0.09±0.02	0.60±0.03	4.97±0.52

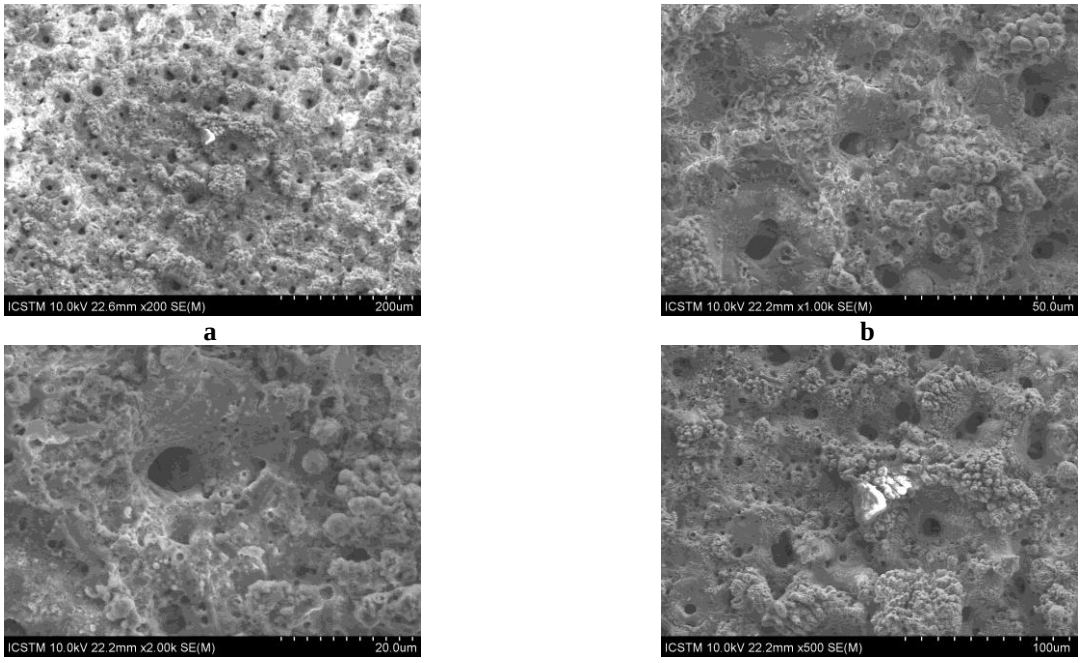

a **b**

c **d**

Figure 6. SEM photomicrographs of S3 sample: a) x200; b) x1000; c) x2000; impurities x500.

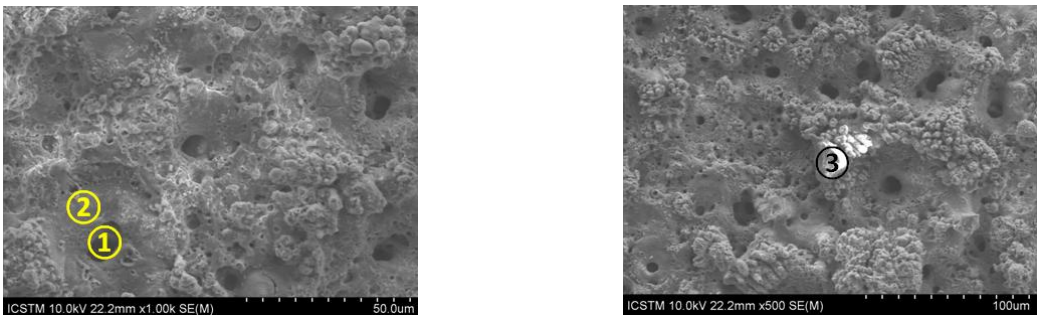

Figure 7. Points of S3 sample analyzed by EDS.

Table 3. The elemental composition determined by FE-SEM-EDS in the studied points of S3 sample, expressed in wt.% ± S.D.%, normalized to 100 wt.%.

Element [wt.%±S.D.%]	P1	P2	P3
Ti	78.47±1.77	37.77±0.65	7.24±0.87
Al	6.83±0.20	45.81±0.23	23.93±0.53
O	14.42±0.64	15.66±0.19	58.86±0.54
Na	0.28±0.07	0.76±0.03	9.97±0.42

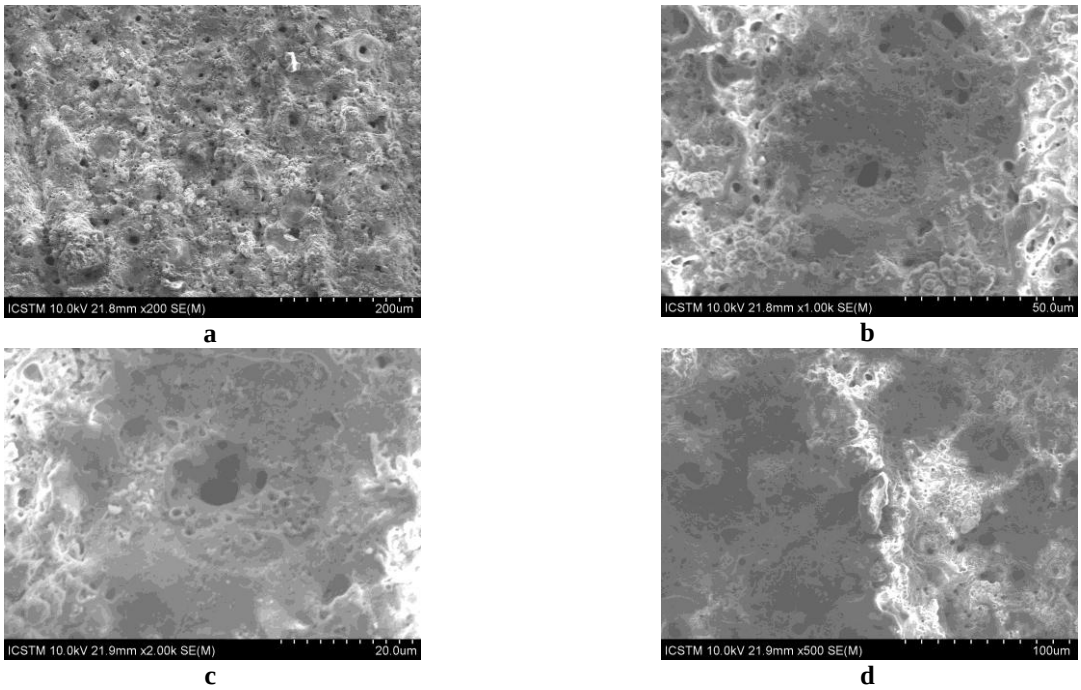

a **b**

c **d**

Figure 8. SEM photomicrographs of S4 sample: a) x200; b) x1000; c) x2000; impurities x500.

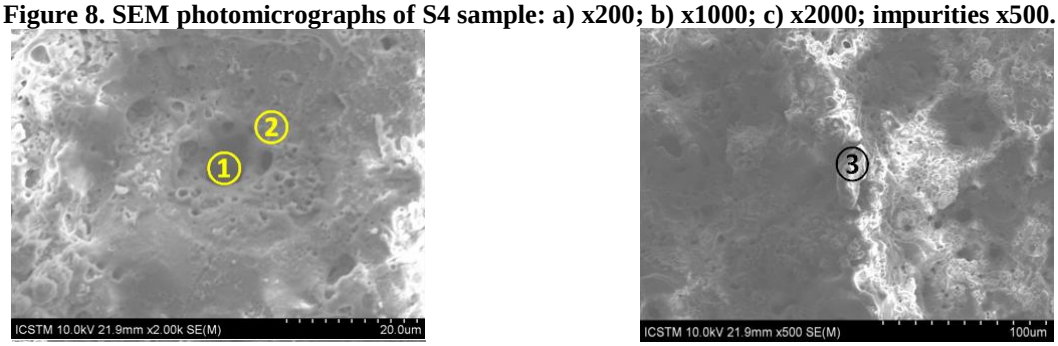

Figure 9. Points of S4 sample analyzed by EDS.

The results obtained by SEM-EDS highlight the dependence of the composition and morphology of the surface layers obtained by PEO on the composition of the electrolyte used.

Low-magnification SEM images show that the oxide layers obtained are porous, with crater-like holes scattered in the film.

Table 4. The elemental composition determined by FE-SEM-EDS in the studied points of S4 sample, expressed in wt.% ± S.D.%, normalized to 100 wt.%.

Element [wt.%±S.D.%]	P1	P2	P3
Ti	57.97±1.69	12.66±0.18	0.92±0.06
Al	17.01±0.21	34.70±0.14	47.18±0.19
O	24.80±0.51	51.49±0.26	50.42±0.26
Na	0.22±0.05	1.15±0.03	1.49±0.02

3.2. XRD ANALYSIS

The qualitative phase analysis was performed with the Integrated X–ray Powder Diffraction Software PDXL 2.4 – qualitative analysis program, using the ICDD PDF4 + 2020 database. Fig. 10 shows the result of the qualitative phase analysis for the PEO layers of samples S1, S2, S3 and S4. The polycrystalline phases identified for samples S1 and S3 (Fig. 10 a) are: titanium aluminum oxide $TiAl_2O_5$ (DB card number 04-011-9497), sodium aluminum oxide $NaAl_6O_9$. (DB card number 04-047-0320), γ – Al_2O_3 (DB card number 00-050-0741) and α – Al_2O_3 (DB card number 04-013-1687). In figure 10 the diffraction lines of 100% intensity: the line (113) for phase α - Al_2O_3 (2ϑ = 43.350) and the line (004) for phase γ – Al_2O_3 (2 ϑ = 45.660) are marked with the symbols (113) α si (004) γ. The integral intensities of lines (113) α and (004) γ were calculated from the diffraction spectra of samples S1 and S3, and the ratio of the relative concentrations of these phases (C α / Cγ) was calculated with the formula from article [12] and is equal to 0.85 for sample S1 and 0.68 for sample S3, respectively. In both samples, the γ–Al_2O_3 phase is in the PEO layers in a higher concentration than the α–Al_2O_3 phase, the value of this concentration decreasing with increasing concentration of sodium aluminate in the electrolyte.

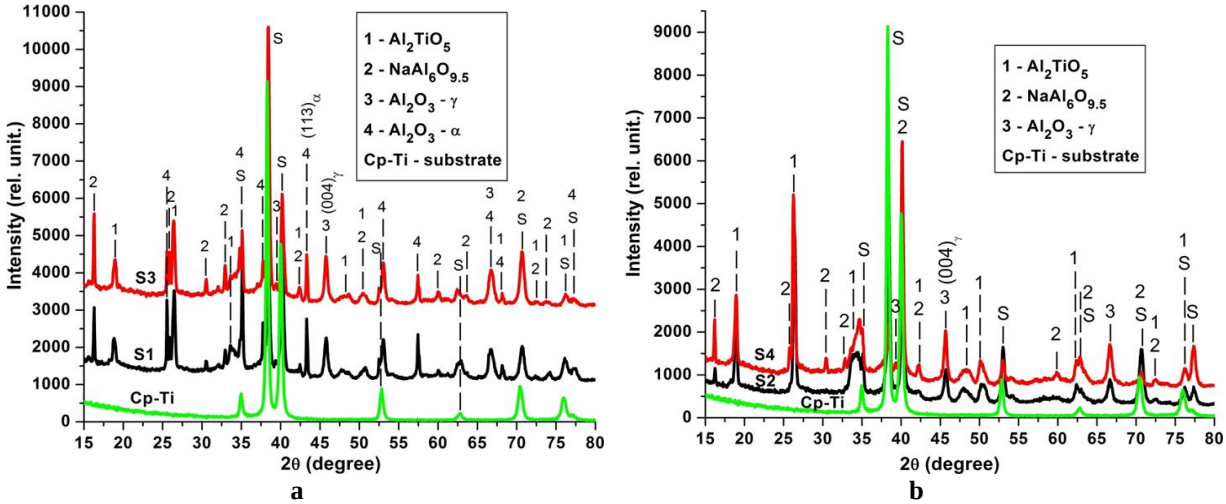

a b

Figure 6. X-ray diffraction patterns of the PEO coatings formed after 5 min process time: 1 - $TiAl_2O_5$ (DB card number 04-011-9497); 2 - *$NaAl_6O_9$.5 (DB card number 00-047-0320); 3- γ-Al_2O_3 (DB card number 00-050-0741); 4 - α-Al_2O_3 (DB card number 04-013-1687); S - Cp-Ti grade 2 (DB card number 04-007-9313):* a) PEO coatings formed after 5 min process time in E1 and E3; b) PEO coatings formed after 5 min process time in E2 and E4 electrolyte.

In the PEO layers of samples S2 and S4 (Fig. 6b) the polycrystalline phase α – Al_2O_3 is missing. In these samples the phases $TiAl_2O_5$ and $NaAl_6O_9$. 5 are majority, and the phase γ

– Al_2O_3 is in a low concentration. The presence of aluminum titanate in a very large amount confirms the hypothesis regarding the role of KOH in favoring the formation of this phase [6]. In these samples, due to the presence in a larger amount of OH- anions, a larger amount of TiO_2 is formed which reacts with Al_2O_3 forming a larger amount of aluminum titanate, compared to samples S1 and S3.

3.3. XPS ANALYSIS

X-ray photoelectron spectroscopic studies were performed to determine the core level binding energies and chemical composition. Survey spectra and high-resolution narrow range XPS spectra for the main elements identified: Al, Ti, O, and Na were recorded for all analyzed samples. Fig. 7 shows a typical survey spectrum that highlights the presence on the surface of the elements of interest Al, Ti, O, Na; C contamination was greatly diminished by bombardment with Ar ions; the spectrum contained the characteristic peaks of the binding energy of the aluminum, titanium, and oxygen core level, indicating the formation of titanium oxide aluminum films. Figs. 8, 9, 10, and 11 show synthetically the information regarding the spectra acquired with high resolution respectively for the peaks Al 2p, O 1s, Ti 2p, Na 1s for the four analyzed samples.

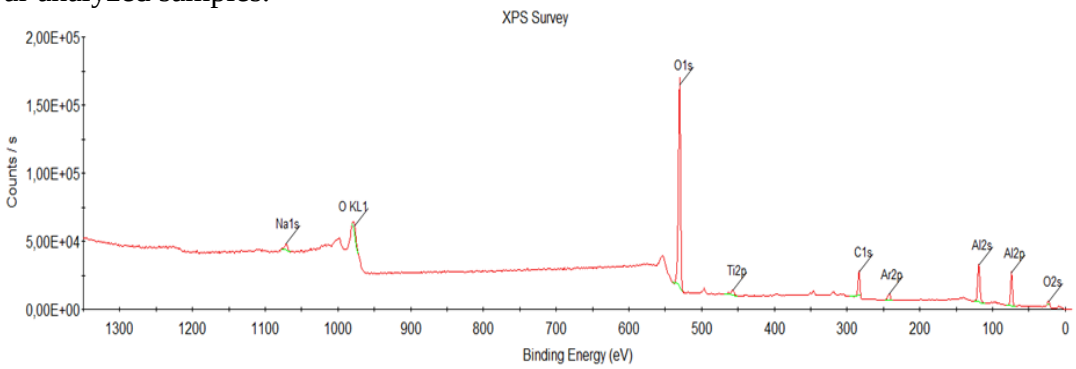

Figure 7. XPS survey spectrum of S1 sample.

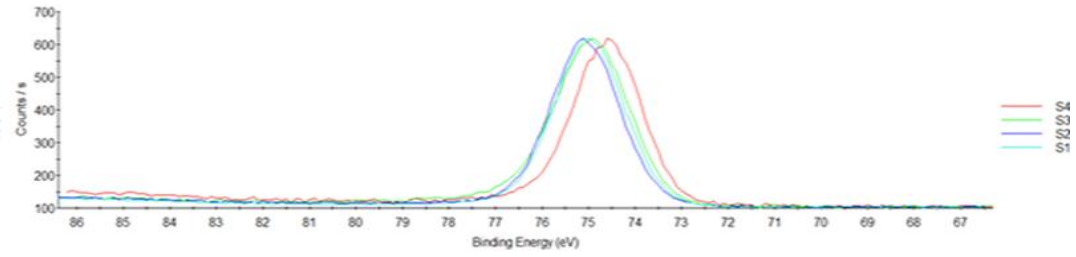

a)

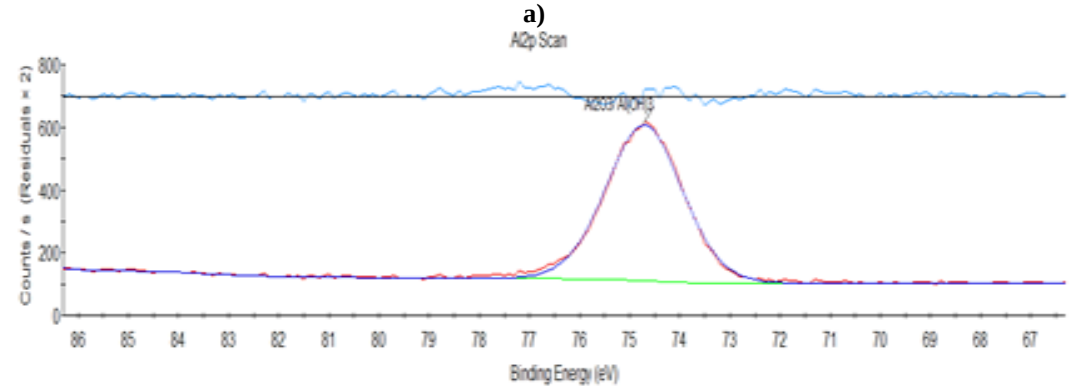

b)

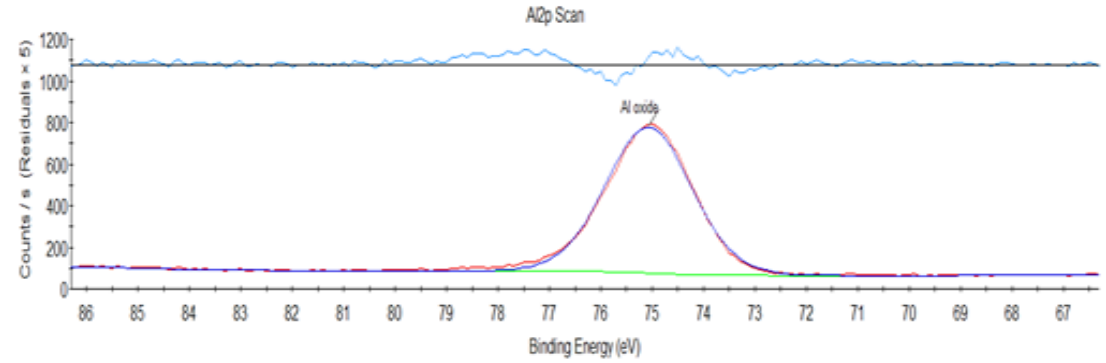

c)

Figure 8. Al 2p peak analysis: a) Overlapping spectra acquired on samples S1, S2, S3, S4 for Al 2p; b) Peak fiting of Al 1s on S4; Eb=74.7eV corresponding toAl_2O_3/$Al(OH)_3$; c) Peak fiting of Al 1s on S3; Eb=75eV corresponding to Al oxide)

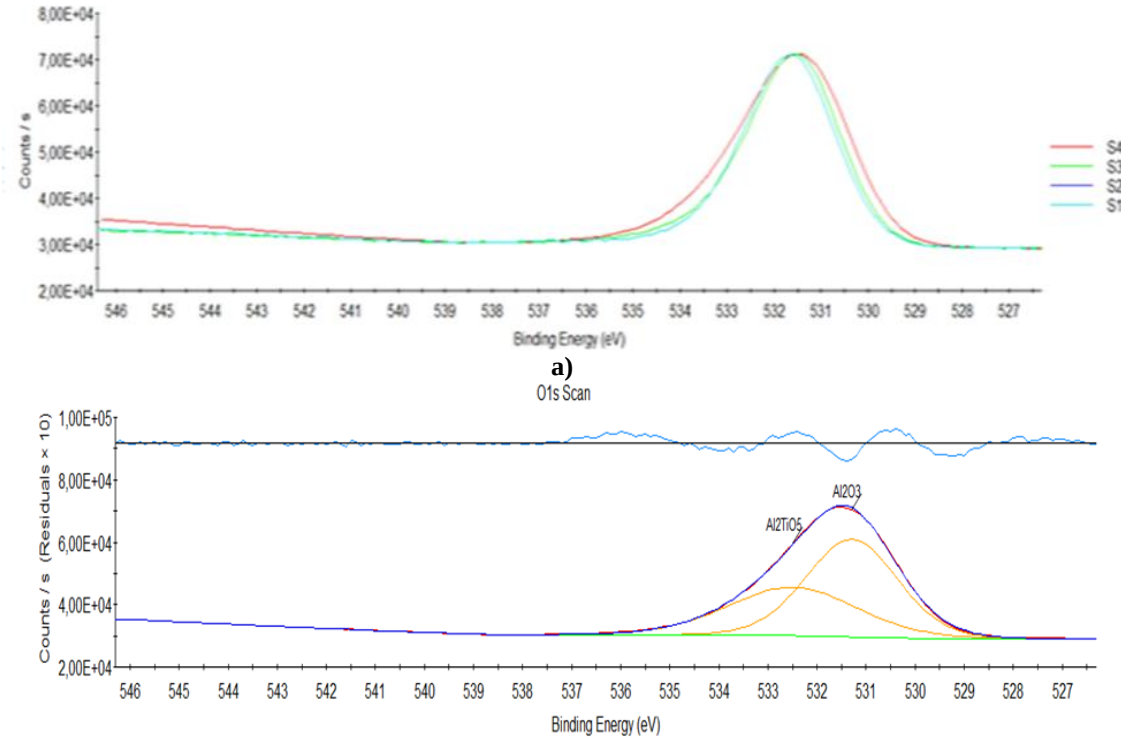

a)

b)

Figure 9. O 1s peak analysis: a) Overlapping spectra acquired on samples S1, S2, S3, S4 for O 1s; b) Peak fiting of O 1s on S4: Eb=531.3eV corresponding to Al_2O_3; Eb=532.5eV corresponding to Al_2TiO_5

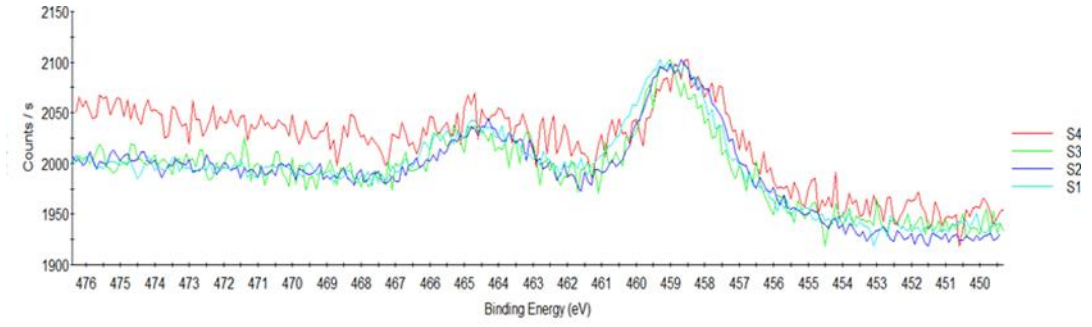

a)

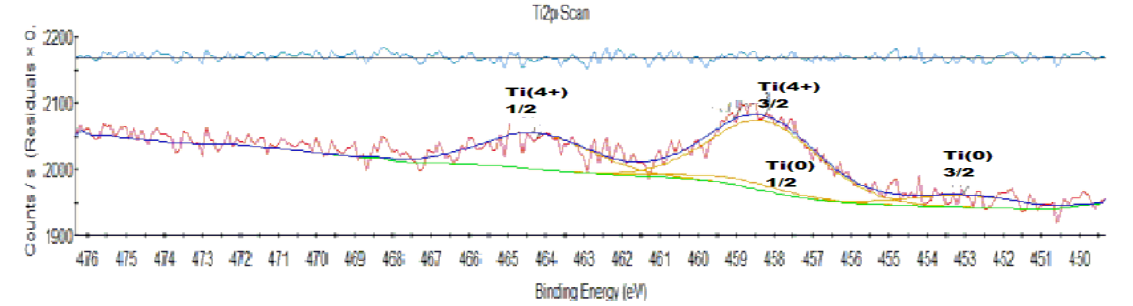

b)

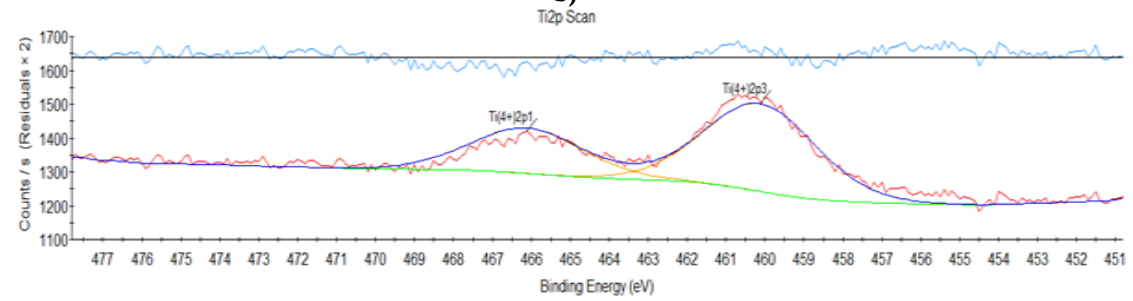

c)

Figure 10. Ti 2p peak analysis: a) Overlapping spectra acquired on samples S1, S2, S3, S4 for Ti 2p; b) Peak fiting of Ti 2p on S4 Ti(0) -14%; Ti(4+) – 86%; c) Peak fiting of Ti2p on S1 Ti $2p^3$-459eV; Ti $2p^1$-465eV.

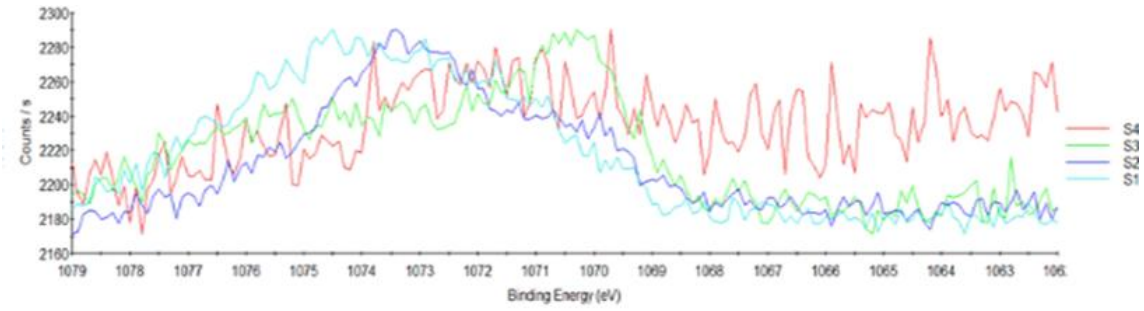

a)

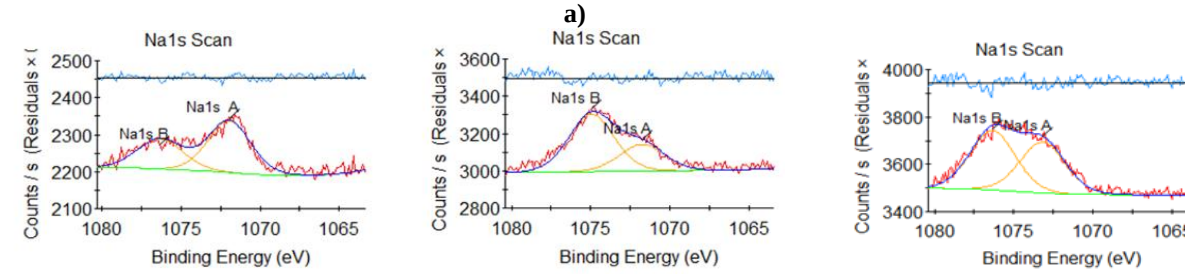

b) c) d)

Figure 11. Na1s peak analysis: a) Overlapping spectra acquired on samples S1, S2, S3, S4 for Na 1s; b) Peak fiting of Na1s on S3, A = $Na_2Ti_3O_7$ – 60%, B = Na_2O – 40%; c) Peak fiting of Na 1s on S2, A = $Na_2Ti_3O_7$ – 38%, B = Na_2O – 62%; d) Peak fiting of Na 1s on S1, A = $Na_2Ti_3O_7$ – 46%, B = Na_2O – 54%.

When overlapping the spectra, the autoscaling option was used to have the same intensity scale for the overlapping spectra. XPS analysis of TiO_2 and Al_2O_3-used as references and of Al_2TiO_5 thin films obtained by SOLGEL [14] showed that the binding energies for Ti $2p^{3/2}$ and Al 2p are in the typical energy range for Ti^{4+} and Al^{3+} ions surrounded by oxigen atoms, there are no significant differences between the different samples. This implies that a straightforward indication of titanate formation cannot be derived merely considering the

binding energies of the two metals, being necessary the analysis of the peak O 1s. The asymmetry of the O 1s peaks observed in Fig. 13 and their width (FWHM~2.8 eV) suggest coexistence of different chemical environments. The peak deconvolution of the O 1s regions demonstrated that the peak was split at least into two bands centered on 531.3 and 532.5 eV (Fig. 13b). These components might represent limited environments associated with Ti-O-Ti and Al-O-Al bonds, respectively, although other hypotheses cannot be excluded, such as the presence in the films of hydroxylated Ti-OH or =Al-OH species, or even mixed Al-O-Ti bonds.

The chemical composition of the coatings was determined from the core level binding energy peak area and the sensitivity factors of the constituent elements of aluminum, oxygen, titanium, and sodium.

Table 5. Element relative concentrations

Sample code	Concentrations [at. %]			
	Al	O	Ti	Na
S1	37.4	59.7	1.6	1.3
S2	40.9	54.5	2.7	1.9
S3	39.4	58.2	1.3	1.1
S4	38.0	58.4	2.6	1.0

3.5. CORROSION BEHAVIOR

The corrosion resistance of the coated Ti substrates was evaluated from potentiodynamic polarization curves in 0.5M aqueous NaCl solution at room temperature. The corresponding values of corrosion potentials (Ecorr) and current densities (icorr) of each sample are listed in Table 6.

Table 6. Results of potentiodynamic polarization tests in 0.5 M NaCl solution at room temperature

Sample code	**Ecor [mV vs. SCE]**	**i [μA/cm^{2}]**	**Corrosion rate [mmpy]**
Substrate Ti	-518	0.820	1.024e-002
S1	-231	0.064	2.249e-003
S2	-26	0.012	4.243e-004
S3	-103	0.027	9.437e-004
S4	61	0.010	3.964e-004

This corrosion behavior of the treated samples, which improves with increasing aluminate concentration in the electrolyte solution, is attributed to the formation of metal oxides on top of the surface, especially aluminum oxides, as indicated by XPS observations. For comparison, the corrosion current densities found in the literature for PEO layers on CP-Ti produced under similar conditions were consistent with or slightly higher than our experimental findings [7-9]. Fig. 12 shows the polarization curves for samples S1, S2, S3, S4 in 0.5 M NaCl aqueous electrolyte. The results obtained by the Tafel slope method are shown in Table 5. To evaluate corrosion behavior, the Tafel slope method was used to determine corrosion potential and corrosion rate.

The polycrystalline phases identified for samples S1 and S3 (Fig. 6a) are titanium aluminum oxide $TiAl_2O_5$, sodium aluminum oxide $NaAl_6O_{9.5}$, γ - Al_2O_3 and α-Al_2O_3. In the PEO layers of samples S2 and S4 (Fig. 6b) the polycrystalline phase α-Al_2O_3 is missing. In these samples the phases $TiAl_2O_5$ and $NaAl_6O_{9.5}$ are majority, and the phase γ - Al_2O_3 is in a low concentration. The PEO process, in the presence of high voltage applied between the anode (sample subjected to treatment) and the cathode, takes place with the participation of ions from the aqueous solution containing $NaAlO_2$ (E1, E3) or $NaAlO_2$ and NaOH (E2, E4) [8,9].

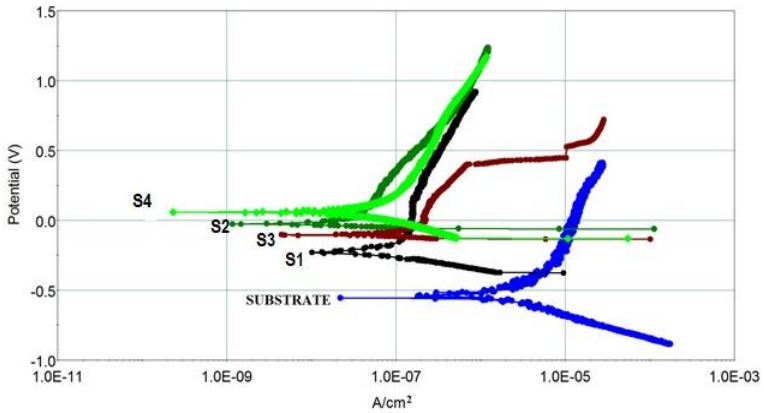

Figure 12. Polarization curves for samples S1, S2, S3, S4 in 0.5 M NaCl aqueous electrolyte.

In the case of aqueous solutions of $NaAlO_2$, the ions participating in the reactions of titanium and aluminum oxide growth are AlO_2^- anions and Ti^{4+} cations formed in the vicinity of the anode under the action of the high electric field formed by applying the applied polarization voltage: $Ti^{4+} + 4AlO_2^- \Leftrightarrow TiO_2 + 2Al_2O_3$; $TiO_2 + Al_2O_3 \rightleftharpoons Al_2TiO_5$. In samples S2, S4, due to the presence in a larger amount of OH^- anions, a larger amount of TiO_2 is formed which reacts with Al_2O_3 forming a larger amount of aluminum titanate, compared to samples S1 and S3. In the case of aqueous solutions of $NaAlO_2$ and NaOH an anodic current is generated due to the OH^- and AlO_2^- anions; when a high voltage is applied to the anode, titanium atoms turn into ions Ti^{4+}, taking place reactions: $Ti^{4+} + 2OH^- + 2H_2O \rightleftharpoons TiO_2 + 2H_3O^+$; $Ti^{4+} + 4AlO_2^- \rightleftharpoons TiO_2 + 2Al_2O_3$.

Further, according to [8], in aqueous alkaline media, $(AlO_2)^-$ anions form aluminum tetrahydroxy ions $[Al(OH)_4]$-; these aluminum ions create an insoluble and low-viscosity gel which covers the surface of the PEO layer; furthermore, Ti4+ ions, partially react with $[Al(OH)_4]$-, resulting TiO_2, Al_2O_3 and $Al(OH)_3$ whereas part of aluminum tetrahydroxy ions are decomposed at the anode under strong electric field, resulting in the end Al_2O_3. At the same time, the lowering of the pH level near the anodic region, due to the polymerization processes, combined with micro-arc discharges result in aluminum hydroxide formation; aluminum hydroxide undergoes thermal transformations to produce alternative phases of aluminum oxide (γ and α). Moreover, the high local temperature resulted from micro-arc discharges along with rapid cooling afterwards, allows phase conversion of aluminum and titanium oxide into aluminum titanate to occur [8]. It should be remembered that due to the higher conductivity in the case of solutions E2, E4, with NaOH, in potentiostatic mode, the current density at the beginning of the film growth process is higher than in the solutions without the addition of NaOH (E1, E3).

It can be noted that increasing the concentration of $NaAlO_2$ in electrolyte and the addition of NaOH led to an increase in the thickness of coating. Indeed, the rise in the concentration of $NaAlO_2$ and the addition of NaOH enhanced the electrolyte conductivity. As a result, the rate of film formation dominated the rate of anodic dissolution, thus forming thicker coating. Increasing $NaAlO_2$ concentration (15 to 20 g/L) led to an enhancement in the compactness and uniformity of the coatings and decreased their structural defects.

4. CONCLUSIONS

Ceramic coatings have been made on CP-Ti grade 2 by PEO treatments in aqueous electrolytic solutions consisting of $NaAlO_2$, at concentrations of 15g/L and 20g/L with or without addition of NaOH - 2g/L, in potentiostatic conditions: U=200V, for 5 min. growth

time, using a unipolar pulsed DC power source with 150 Hz frequency . The thickness of the ceramic layers obtained are in the field of 12-36 μm; by increasing the concentration of $NaAlO_2$ and by adding NaOH, coatings with higher and more uniform thickness are obtained. The coatings obtained are porous, with crater-like holes and microsized particles scattered in the film. The polycrystalline phases identified for samples without adaus by NaOH are: titanium aluminum oxide $TiAl_2O_5$, sodium aluminum oxide $NaAl_6O_9$, $\gamma - Al_2O_3$ and $\alpha - Al_2O_3$; the $\gamma - Al_2O_3$ phase is in the PEO layers in a higher concentration than the $\alpha - Al_2O_3$ phase, the value of this concentration decreasing with increasing concentration of sodium aluminate in the electrolyte. In the PEO layers of samples with adaus by NaOH the polycrystalline phase $\alpha - Al_2O_3$ is missing and the phases $TiAl_2O_5$ and $NaAl_6O_{9.5}$ are majority; the phase $\gamma - Al_2O_3$ is in a low concentration. In the case of aqueous solutions of $NaAlO_2$, the ions participating in the reactions of titanium and aluminum oxide growth are AlO_2^- anions and Ti^{4+} cations formed in the vicinity of the anode under the action of the high electric field formed by applying the applied polarization voltage; in the case of aqueous solutions of $NaAlO_2$ and NaOH, due to the presence in a larger amount of OH^- anions, a larger amount of TiO_2 is formed which reacts with Al_2O_3 forming a larger amount of aluminum titanate.

The results obtained by the Tafel slope method regarding the corrosion behavior of the PEO-treated samples compared to an untreated sample show a decrease in the corrosion rate by one or two orders of magnitude as a result of the applied treatment, as well as a significant shift in the potential of corrosion towards more positive values; the sample treated in aqueous solution of $NaAlO_2$, at concentrations of 20 g/L, with addition of NaOH - 2g/L has. the best corrosion behavior.

Acknowledgement: *This work was supported by the Ministry of Research, Innovation and Digitization through Project no. 43PFE/30.12.2021.*

REFERENCES

[1] Bignon, Q., Martin, F., et al., *Corrosion Science*, **150**, 32, 2018.
[2] Raj, B., Kamachi Mudali, U., *Surface Engineering*, **19**(5), 321, 2003.
[3] Fattah-Alhosseini, A., Keshavarz, M. K., Molaei, M., Gashti, S.O., *Metallurgical and Materials Transactions A*, **49,** 4966, 2018.
[4] Yerokhin, A.L., Leyland, A., Matthews, A., *Applied Surface Science*, **200**, 172, 2002.
[5] Singh, N., Master Thesis Synthesis, *Sintering and Characterization Of Al2o3-13 Wt. % Tio2 Composite Powder Prepared By Polymer Assisted Coprecipitation Route*, National Institute Of Technology, Rourkela, India, 2014.
[6] Shokouhfar, M., Dehghanian, C., Baradaran, A., *Applied Surface Science*, **257**(7), 2617, 2011.
[7] Molaei, M., Fattah-Alhosseini, A, Gashti, S.O., *Metallurgical and Materials Transactions A*, **49**(A), 369, 2018.
[8] Malinovschi, V., Marin, A., et al., *Surface and Coatings Technology*, **418,** 127240, 2021.
[9] Malinovschi, V., Marin, A. H., et al., *Coatings*, **12**(1), 29, 2022.
[10] American Society for Metals, *Metals Handbook, 8th Edition, vol.8, Metallography, Structures and Phase Diagrams*, prepared under direction of the ASM HANDBOOK COMMITTEE, September 1973.
[11] Malinovschi, V., Marin, A., Moga, S., Negrea, D., *Surface and Coatings Technology*, **253**, 194, 2014.
[12] Xue, W., Deng, Z., Lai Y., Chen, R., *Journal of the American Ceramic Society*, **81**(5), 1365, 1998.
[13] Shokouhfar, M., Dehghanian, C., Baradaran, A., *Applied Surface Science*, **257**(1), 2617, 2011.
[14] Innocenzi, P., Martucci, A., Armelao, L., Licoccia, S., Di Vona, M. L., Traversa, E., *Chemistry of Materials*, **12**, 517, 2000.